Contents lists available at ScienceDirect

Nuclear Inst. and Methods in Physics Research, B

journal homepage: www.elsevier.com/locate/nimb

L- and M-subshell ionization cross-sections of heavy atoms by electron and proton impact

C.C. Montanari [a,*], S. Segui [b], A.M.P. Mendez [a], D.M. Mitnik [a]

[a] Instituto de Astronomía y Física del Espacio, CONICET – UBA, Intendente Guirales s/n, Ciudad Universitaria, 1428 Buenos Aires, Argentina
[b] Instituto de Física Enrique Gaviola, CONICET – UNC. Av. Medina Allende s/n, Ciudad Universitaria, 5000 Córdoba, Argentina

ARTICLE INFO

Keywords:
Inner shell ionization
Electron
Proton

ABSTRACT

Inner-shell ionization has many applications related to material analysis. However, full theoretical calculations in heavy multielectronic atoms are scarce. In this contribution, we assess proton and electron impact L_i and M_i-subshell ionization cross-sections of heavy targets ($72 \leq Z \leq 83$) using two theoretical models. These calculations are based on the Distorted Plane Wave Born Approximation for electron impact and the shellwise local plasma approximation for the proton impact, combined with relativistic calculations of these deep subshells wave functions and binding energies. We analyze the L-shell ionization of W, Au, and Bi and the M-shell of Hf, Ta, W, Re, Os, Pt, Au, Pb, and Bi. Present values are compared with available experimental data from the literature, with disparate agreement. The convergence of proton and electron impact cross-sections at high-impact velocities is also discussed.

1. Introduction

Despite the long history of atomic collision physics, different tasks remain to be completed, especially in determining ionization cross-sections. From a theoretical point of view, the description of inner shells of multielectronic targets is far from the hypothesis of a hydrogenic target with a single active electron in a central potential. The wave functions and binding energies of these targets are obtained by solving the Dirac equation, which includes the spin–orbit split in energy. Experimentally, the multiple bound shells and the many-decay paths to be considered hamper the accurate assessment of the ionization cross sections. These are obtained indirectly from measured X-ray production cross-sections, and the conversion to ionization cross-sections involves a series of relaxation parameters [1–4].

One of the most employed theories for ion-beam ionization of deep shells is the ECPSSR [5] and its evolution ECUSAR [3], which covers an extended energy range and is the usual input in PIXE codes. A recent review by Lapicki [6] on L-shell ionization by protons states ECUSAR as the most accurate model to describe the available data. Different compilations of experimental data are available, mainly for X-ray production cross sections, such as Miranda and Lapicki [7], Llovet [2], Pajek [3], and recently by Sanjiv Puri group [8]. However, theoretical–experimental differences remain present [3], whereby independent and *ab initio* models are helpful.

The current work presents electron and proton impact full theoretical results for the different L_i and M_i ionization cross-section of Hf, Ta, W, Re, Os, Pt, Au, Pb, and Bi with two different models: a many-electron description of target ionization by proton impact employing the shellwise local plasma approximation (SLPA) [9,10] and a complementary assessment of ionization cross sections for energetic electrons using Distorted Plane Wave Born Approximation (DWBA) [11,12] in the same range of projectile velocities. The convergence of electron to proton impact ionization cross-sections is well-known and experimentally confirmed for total cross-sections (i.e., for impact velocities around 4 a.u for Xe target [13]); however, the behavior for deep subshells could be different. The objective is to evaluate these detailed calculations, comparing proton and electron impact cross-sections to study their thresholds and convergence. We also test the theoretical results with the corresponding experimental data. This work is the first step in a deeper study involving the relaxation parameters and the production of the X-ray production cross-sections.

The paper is organized as follows: we briefly describe the theoretical models in Section 2. The results obtained are analyzed in Section 3, and concluding remarks are outlined in Section 4.

* Corresponding author.
E-mail addresses: mclaudia@iafe.uba.ar (C.C. Montanari), silvina.segui@mi.unc.edu.ar (S. Segui), alemendez@iafe.uba.ar (A.M.P. Mendez), dmitnik@df.uba.ar (D.M. Mitnik).

https://doi.org/10.1016/j.nimb.2024.165440
Received 6 January 2024; Received in revised form 7 June 2024; Accepted 10 June 2024

Table 1
Binding energies (in a.u.) of each subshell obtained by the present HULLAC calculations.

Z	L_1	L_2	L_3	M_1	M_2	M_3	M_4	M_5
72	409.0	390.3	346.4	93.55	85.40	75.97	62.14	60.11
73	423.9	404.5	357.8	97.63	89.27	79.14	65.11	62.94
74	439.4	419.8	369.9	101.5	92.91	82.07	67.64	65.32
75	455.8	435.6	382.4	106.0	97.23	85.59	70.84	68.36
76	471.1	450.3	393.9	109.9	100.9	88.54	73.56	70.92
78	510.1	487.8	425.0	121.1	111.2	97.20	80.92	77.98
79	522.0	499.6	432.0	123.65	114.0	98.95	83.15	79.97
82	577.5	553.7	473.0	139.4	129.1	111.0	94.06	90.28
83	597.0	572.5	487.2	145.0	134.4	115.2	98.07	94.05

Table 2
Present HULLAC mean velocities (in a.u.) of each subshell.

Z	L_1	L_2	L_3	M_1	M_2	M_3	M_4	M_5
72	24.8	34.7	31.0	12.8	15.5	14.5	17.9	17.2
73	25.4	35.2	31.3	13.1	15.9	14.8	18.0	17.6
74	27.1	35.3	31.3	13.3	16.3	15.0	18.3	17.8
75	26.1	36.6	32.3	13.6	16.7	15.4	18.7	18.2
76	26.6	32.8	37.4	13.7	17.00	15.7	19.0	18.5
78	27.8	38.8	33.8	14.2	17.6	16.3	19.6	19.2
79	27.6	38.7	33.6	14.6	17.9	16.4	18.9	19.3
82	29.0	40.9	35.00	15.4	18.9	17.1	20.8	20.2
83	29.4	41.5	35.4	15.7	19.3	17.4	21.2	20.6

2. Theoretical models

2.1. SLPA-HULLAC calculations for proton impact

The SLPA [9] is a perturbative model to predict the ion-impact ionization probabilities within the dielectric formalism. It is a many-particle model, with each subshell of target electrons being described as an inhomogeneous density of electrons with an ionization gap of energy. This model is expected to be accurate for impact velocities greater or equal to that of the target electrons. The only inputs for the SLPA calculations are the binding energies and wave functions of the atomic subshells of the ground state. These values are obtained as fully relativistic solutions by means of the many-electron Dirac equation implemented in the HULLAC code package [14]. The calculations are based on the first-order perturbation theory with a central field, including Breit interaction and quantum electrodynamics corrections. The combination of the SLPA and HULLAC has been employed in total L and M-shell calculations in the past [10], and they have been improved more recently to get the different L and M subshell ionization cross-sections by heavy ions [15–17]. Table 1 displays the present results for the L_i and M_i binding energies(in atomic units) of Hf, Ta, W, Re, Os, Pt, Au, Pb, and Bi. The binding energies obtained, which include spin–orbit splitting, agree within 2% with the compiled experimental values [18] for these deep shells. Present HULLAC mean velocities of each subshell, obtained from the Fourier transform of each wave function, are displayed in Table 2. The binding energies and mean velocities are useful parameters for evaluating the ionization cross-sections, thresholds, convergence at high energies, and the validity range of each model.

2.2. DWBA calculations for electron impact

There exist different approaches to calculate electron ionization cross sections, including empirical formulas and first-principles derivations [2]. The former have been widely used for specific applications but are limited to certain energy ranges and atomic numbers for which experimental data are available. On the other hand, *ab initio* calculations have benefited from the access to computation facilities that allow the assessment of increasingly sophisticated models. In this work, we use an analytical expression for the ionization cross-section based on a semi-relativistic distorted-wave Born approximation (DWBA) [11, 19] combined with the plane-wave Born approximation (PWBA) to calculate ionization cross-sections for electrons. In the DWBA, the atomic wave functions are described within the independent-electron approximation, i.e., the ionization process involves a single (active) target electron. One-electron orbitals are obtained from the Dirac equation using self-consistent Dirac–Hartree–Fock–Slater (DHFS) potentials. The electron projectile is described using plane waves distorted by the atomic potential. In that range, this approximation is feasible for energies up to approximately 16 times the ionization energy of the considered shell due to convergence issues, and only the longitudinal part of the interaction between the projectile and the active electron is considered. For higher projectile energies, the ionization cross-section is calculated using plane waves, and the transverse part of the interaction is included.

In Fig. 1, we compare the present DHFS and HULLAC binding energies from $1s$ to $5p\pm$ for the first five post-lanthanum elements. The $4f\pm$ electrons in these solids belong to a sub-valence shell located just below the conduction band, and they are less bounded than the $5s$ and $5p\pm$, as can be noted in this figure. The theoretical binding energies are also compared in Fig. 1 with the experimental values in solids compiled in Ref. [18]. The agreement of theoretical and experimental results is excellent for the L and M shells of interest here. It is worth mentioning that these relativistic results agree within 2% with the experimental data, which significantly improves non-relativistic results based on the Hartree–Fock method [20] that show discrepancies up to about 13%. An example of the improvements obtained in the binding energies when using a relativistic framework instead of a non-relativistic one is shown in Fig. 2 of [21] for Hf. For the outer shells, the theory-experiment differences increase; however, there is still good agreement between the two relativistic calculations (HULLAC and DHFS).

3. Results and discussions

In Fig. 2, we show the ionization cross-sections as a function of the projectile velocity v of the different L_i-subshells, and the total L-shell values of tungsten by proton and electron impact using the SLPA and the DWBA. The corresponding calculations for gold and bismuth are shown in Fig. 3. For electron impact, the DWBA shows the ionization threshold at impact velocities around or just below the mean velocity of the subshell (see Table 2). For proton impact, the similarity of the L_1 and L_2 SLPA cross-sections is noticeable. This result could be ascribed to the fact that the L_1 and L_2 subshells have the same number of electrons in the orbital and close binding energies, as shown in Table 1. Note that in this range of velocities, proton and electron ionization cross-section curves are not yet convergent.

Selected sets of experimental data are included in the figures. For protons, we have used the compilation made by Miranda and Lapicki [7], who reviewed most of the work done on this shell ionization cross-sections by various authors. We show the subshells and total shell data from this compilation for W and total L shell data for Au and Bi. The experimental uncertainties reported for these data range from 8 to 14%. For Au, we have also included total and subshell measurements by Hardt and Watson [23], with relative errors of 5%–10%. In the case of electron impact, we have included measurements by Chang [22] for W, Rahangdale et al. for Au [24], and Barros et al. for Au [25] and Bi [26]. The reported relative errors in these works are 15%, 10%–15%, 7%–8%, and 5%–6%, respectively. It is worth mentioning that these experimental data are obtained indirectly from characteristic X-ray measurements and, in general, they are affected by the choice of the different relaxation parameters (e.g., fluorescence yields and Coster–Kronig transition probabilities) used in the conversion from X-ray production to ionization cross-sections. The dispersion found among different sets of parameters may introduce variations in the converted quantities as large as 30%, depending on the combination of databases [1,4,23,26]. This issue is evinced by the data for Au provided

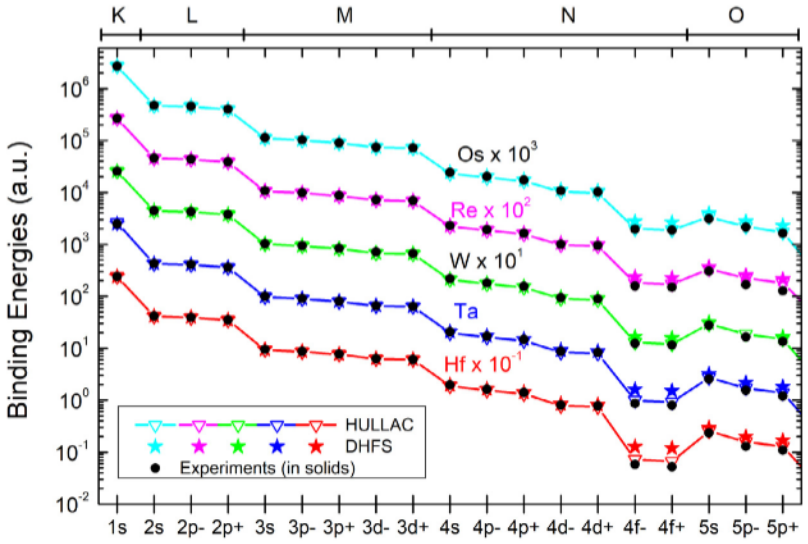

Fig. 1. Binding energies of atoms with $72 \leq Z \leq 76$ by using HULLAC (open triangle and solid line) and DHFS (filled stars). Experimental data [18] are included as solid bullets.

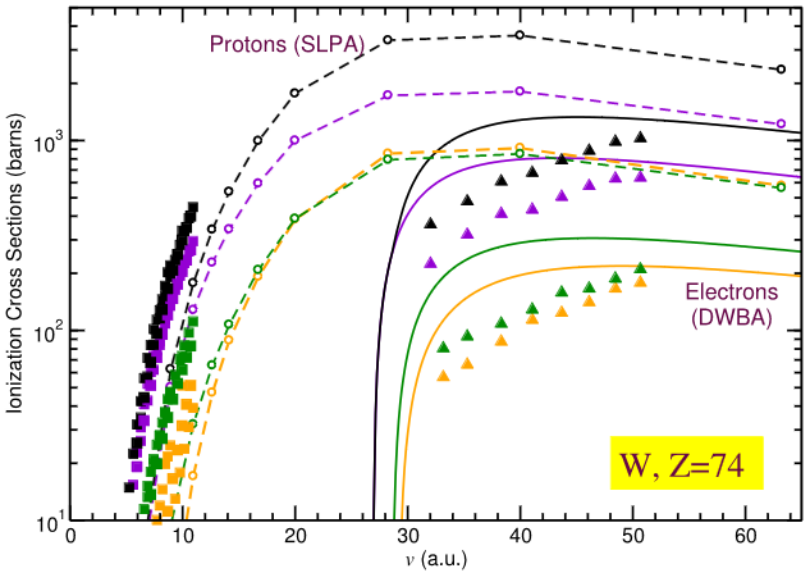

Fig. 2. L-shell ionization cross-sections of W as a function of the impact velocity v: subshells L_1 (orange), L_2 (green) and L_3 (violet), and total L (black) for protons calculated with SLPA (hollow circles+dashed lines) and electrons calculated with DWBA (continuous lines). Experimental data for protons: squares, compiled by Miranda and Lapicki [7]. Experimental data for electrons: triangles, Chang [22].

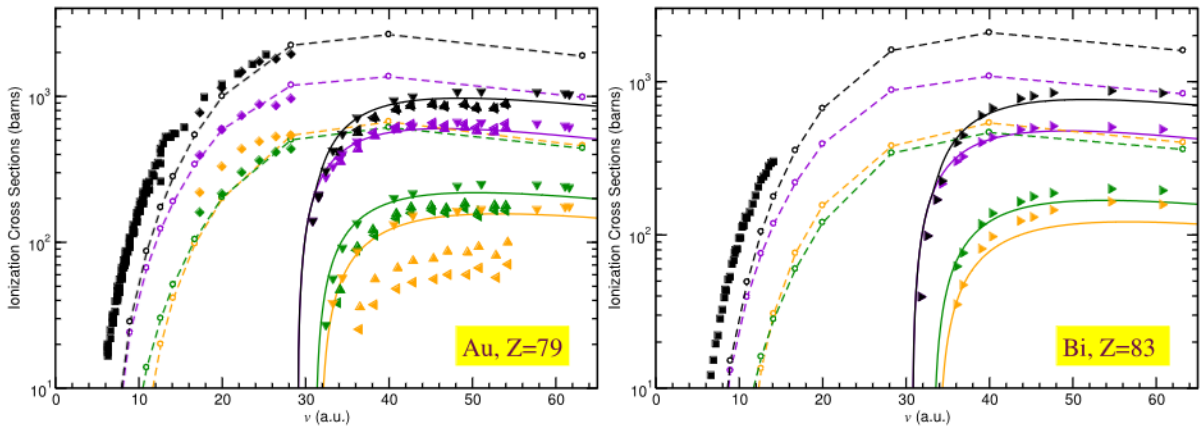

Fig. 3. Similar to Fig. 2 for Au (left) and Bi (right) targets. Experimental data for protons: diamonds, Hardt [23]; squares, data compiled by Miranda and Lapicki [7] (only data for total L-shell included). Experimental data for electrons: triangles up and left, Rahangdale et al. [24], triangles down, Barros et al. [25], triangles right, Barros et al. [26].

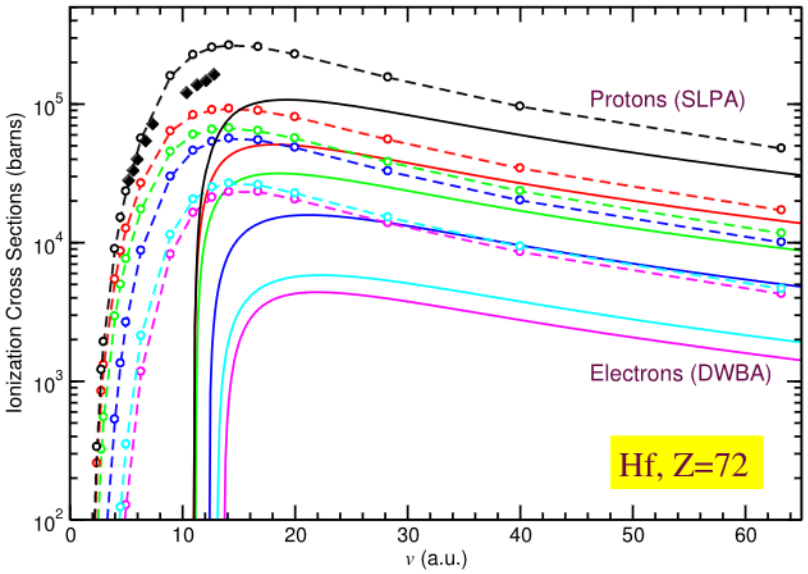

Fig. 4. M-shell ionization cross-sections of Hf as a function of the impact velocity v: M_1 (magenta), M_2 (cyan), M_3 (blue), M_4 (green), M_5 (red) subshells and total M (black) for protons calculated with SLPA (symbols+dashed lines) and electrons calculated with DWBA (continuous lines). Experimental data for protons: diamonds, Pajek et al. [27].

Table 3
Electron to proton L- and M-(sub)shells ionization cross-section ratios at a projectile velocity of $v = 63.24$ a.u.

Z	L_1	L_2	L_3	L_{tot}	M_1	M_2	M_3	M_4	M_5	M_{tot}
72	0.34	0.47	0.54	0.47	0.34	0.42	0.50	0.78	0.83	0.66
73	0.33	0.46	0.54	0.47	0.34	0.42	0.50	0.77	0.83	0.66
74	0.34	0.47	0.54	0.47	0.34	0.42	0.50	0.76	0.82	0.66
75	0.33	0.46	0.53	0.46	0.34	0.42	0.50	0.76	0.81	0.65
76	0.33	0.46	0.52	0.46	0.33	0.42	0.49	0.74	0.80	0.64
78	0.32	0.45	0.52	0.45	0.33	0.41	0.49	0.73	0.79	0.63
79	0.32	0.45	0.52	0.46	0.33	0.41	0.49	0.73	0.78	0.63
82	0.28	0.45	0.52	0.47	0.33	0.41	0.49	0.72	0.77	0.62
83	0.29	0.44	0.52	0.44	0.33	0.41	0.48	0.72	0.77	0.62

by Rahangdale et al. (triangles up and left), who give two sets of values for the ionization cross-sections using two sets of relaxation parameters. For proton impact, the data reported in Ref. [7] correspond to velocities below the range of validity of the SLPA mentioned in Section 2. This would explain the differences observed in the low-velocity range for the three elements considered, while the data from Ref. [23] for Au show a good agreement for velocities higher than 20 a.u.

In Figs. 4 to 6, the SLPA (proton impact) and DWBA (electron impact) cross-sections for M shells of most elements from Hf ($Z = 72$) to Bi ($Z = 83$) are displayed. We can observe again that the thresholds for electron impact ionization of the M_i-subshells are close to the velocity of the electrons in the subshell, as displayed in Table 2.

Although the high-energy convergence of proton and electron impact cross-sections seems to be outside the range of velocities considered here, the confluence of the results at high velocities is clear for the less bound M_4 and M_5 subshell. To quantify this trend, we present in Table 3 the ratio of electron to proton cross-sections at the same velocity, corresponding to 100 MeV protons and ~ 54 keV electrons, for all L and M subshells. Noticeably, the ratios for the L_i and M_i subshells are similar for $i = 1 - 3$, although the binding energies and mean velocities are very different.

Experimental ionization cross-sections of the M-shell are very scarce. Most of the data are published as X-ray production cross-sections and the comparison with the theoretical ionization cross-section values is hampered by a more complex conversion procedure than for L-shell due to the many possibilities of producing a vacancy in a given M-subshell and the associated relaxation parameters involved. To our knowledge, no electron impact M-shell ionization cross-sections of these targets have been published in the energy range considered here. For proton impact, a thorough study was published by Pajek et al. [3], including measurements of X-ray production cross-sections for all the elements considered here, total ionization cross-sections, and the results by the ECPSSR. We include in Figs. 4 to 6 the comparison with the experimental data by Pajek and collaborators [3,27] and Ishii et al. [28]. The uncertainties reported by Pajek et al. are 12%–15%, except for Os (9%) and Bi (10%), while Ishii et al. reported 10%–20% for their data. It can be noted that the agreement with data in Ref. [28] for Au and in Ref. [3] for Ta, W, Re, Os, Pt, Au, and Bi is reasonable. The values in Ref. [27] for Hf, W, and Ta are overestimated by the SLPA, while for Au, they agree rather well. As discussed above for L-shells, and also as pointed out in Ref. [27], the adopted M-shell fluorescence yields and Coster–Kronig factors are crucial. Differences using transitions tabulated in Chen et al. [29] and in McGuire [30] are observed for Hf, Ta, and W, and not for the heavier targets [3]. It is worth mentioning that the ionization cross-sections in Ref. [3] use yields from [30], while Ref. [27] uses values reported in [29]. These differences raise the debate about fluorescence yields and X-ray production cross-sections and their conversion to ionization cross-sections, which evince the importance of independent full theoretical calculations.

4. Conclusions

This work presents full theoretical L and M-shell ionization cross-sections of heavy targets by proton and electron impact by means of the SLPA and DWBA, respectively. The total M-shell ionization cross-sections for protons converge to the electron-impact ones at $v \geq 60$ a.u. For electron impact, the L_i ionization cross-sections describe the experimental data well overall. No M_i experimental ionization cross-sections were found in the literature below 60 keV for the elements studied here. For proton impact, the SLPA's agreement with L-shell measurements is good only for impact velocities above 20 a.u., as expected due to this model's validity range. For M-shell ionization, the comparison is rather good. Differences in experimental data due to relaxation parameters, such as fluorescence yields and Coster–Kronig factors, are mentioned. These parameters depend only on the target, so comparison for different projectiles could be helpful and will be addressed in future work.

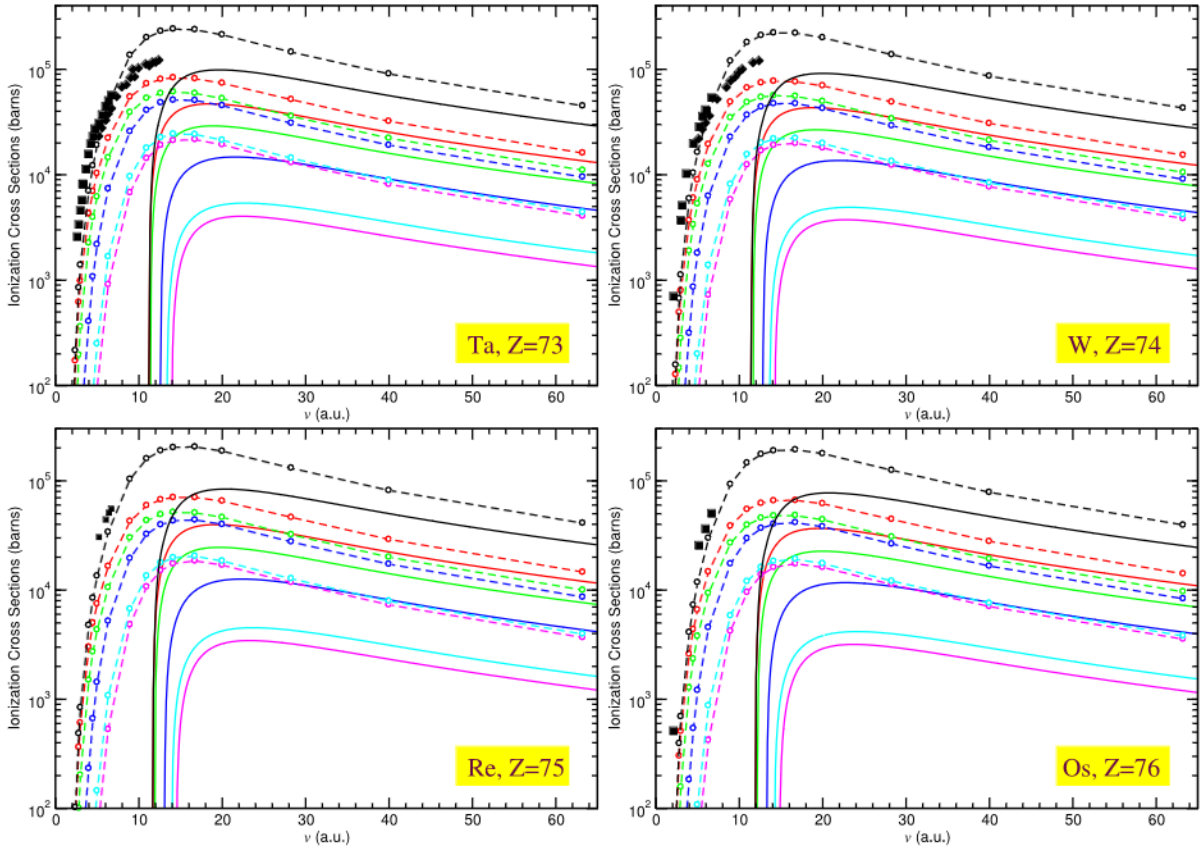

Fig. 5. Similar to Fig. 4 for Ta, W, Re, Os targets. Experimental data for protons: squares, Pajek et al. [3]; diamonds, Pajek et al. [27].

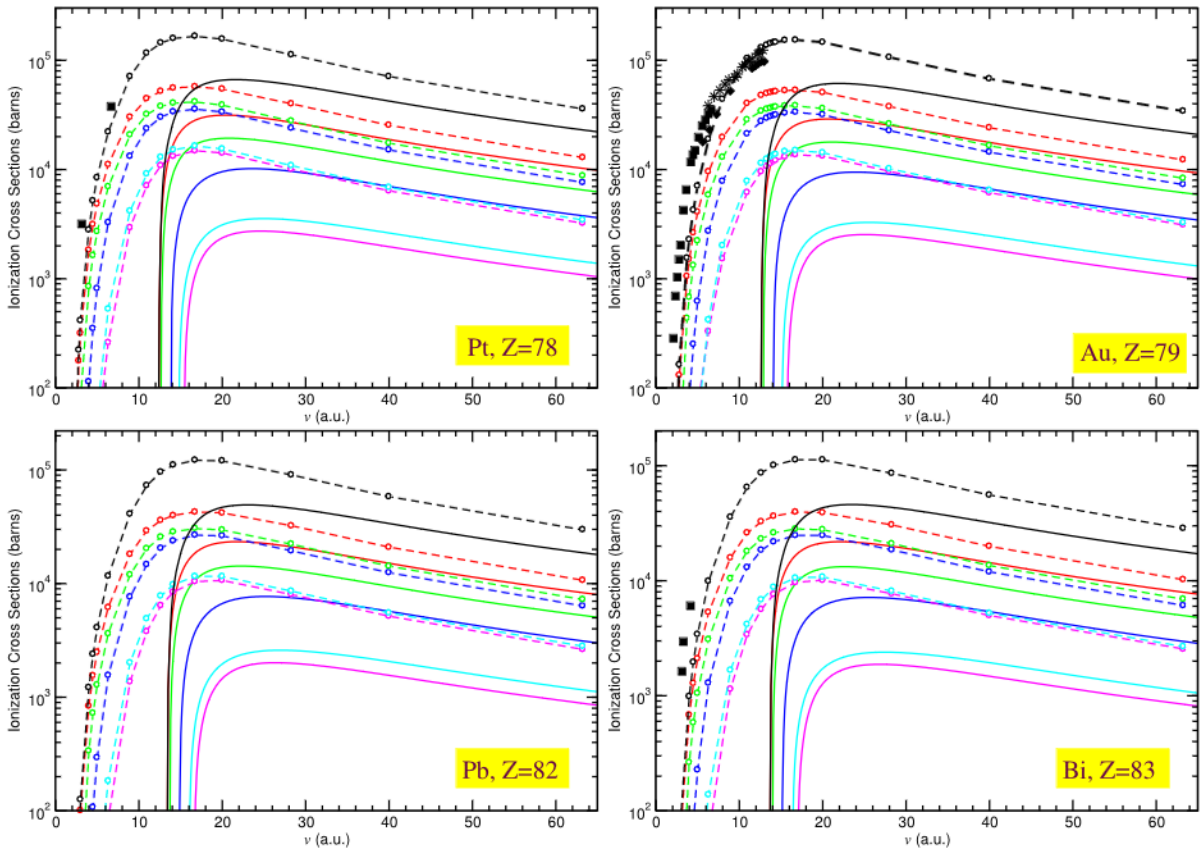

Fig. 6. Similar to Fig. 4 for Pt, Au, Pb and Bi targets. Experimental data for protons: squares, Pajek et al. [3]; diamonds, Pajek et al. [27]; stars, Ishii et al. [28].

Declaration of competing interest

none

Acknowledgments

We are grateful to Prof. J. M. Fernández-Varea and Prof. M. Dingfelder for useful discussions in the development of this work. The present work was partially supported by the following projects: PIP11220200102421CO and PIP11220210100141CO by CONICET, Argentina, and PICT-2020-SERIE A-01931 by the ANPCyT, Argentina.

References

[1] J.M. Fernández-Varea, S. Segui, M. Dingfelder, Lα, Lβ, and Lγ x-ray production cross sections of Hf, Ta, W, Re, Os, Au, Pb, and Bi by electron impact: Comparison of distorted-wave calculations with experiment, Phys. Rev. A 83 (2011) 022702, http://dx.doi.org/10.1103/PhysRevA.83.022702.

[2] X. Llovet, C.J. Powell, F. Salvat, A. Jablonski, Cross sections for inner-shell ionization by electron impact, J. Phys. Chem. Ref. Data 43 (1) (2014) 013102, http://dx.doi.org/10.1063/1.4832851.

[3] M. Pajek, D. Banaś, J. Braziewicz, M. Czarnota, A. Bieńkowski, M. Jaskół a, A. Korman, D. Trautmann, G. Lapicki, M-shell ionization of heavy elements by 0.1-1.0 MeV/amu ^{1,2}H and ^{3,4}He ions, Phys. Rev. A 73 (2006) 012709, http://dx.doi.org/10.1103/PhysRevA.73.012709.

[4] A. Carreras, G. Castellano, S. Segui, J. Trincavelli, Experimental x-ray production cross sections for the M_3, M_4, and M_5 subshells of Pt and Au by electron impact, Phys. Rev. A 102 (2020) 012817, http://dx.doi.org/10.1103/PhysRevA.102.012817.

[5] W. Brandt, G. Lapicki, Energy-loss effect in inner-shell Coulomb ionization by heavy charged particles, Phys. Rev. A 23 (1981) 1717–1729, http://dx.doi.org/10.1103/PhysRevA.23.1717.

[6] G. Lapicki, The status of theoretical L-shell x-ray production cross sections by protons based on their revised universal empirical fit, Nucl. Instrum. Methods Phys. Res. B 467 (2020) 123–129, http://dx.doi.org/10.1016/j.nimb.2019.12.008, URL https://www.sciencedirect.com/science/article/pii/S0168583X19308171.

[7] J. Miranda, G. Lapicki, Experimental cross sections for L-shell x-ray production and ionization by protons, At. Data Nucl. Data Tables 100 (2014) 651, http://dx.doi.org/10.1016/j.adt.2013.07.003.

[8] B. Singh, Shehla, S. Puri, A review, tabulation, and parameterization of M-series X-Ray production cross sections for proton and helium ion impact, J. Phys. Chem. Ref. Data 50 (4) (2021) 043106, http://dx.doi.org/10.1063/5.0058390, arXiv:https://pubs.aip.org/aip/jpr/article-pdf/doi/10.1063/5.0058390/14794979/043106_1_online.pdf.

[9] C.C. Montanari, J.E. Miraglia, The dielectric formalism for inelastic processes in high-energy ion–matter collisions, in: D. Belkic (Ed.), in: Advances in Quantum Chemistry: Theory of Heavy Ion Collision Physics in Hadron Therapy, vol. 2, Elsevier, New York, 2013, pp. 165–201, http://dx.doi.org/10.1016/B978-0-12-396455-7.00007-8.

[10] C.C. Montanari, D.M. Mitnik, J.E. Miraglia, A collective model for inner shell ionization of very heavy targets, Rad. Eff. Def. Solids 166 (2011) 338, http://dx.doi.org/10.1080/10420150.2011.572284.

[11] S. Segui, M. Dingfelder, F. Salvat, Distorted-wave calculation of cross sections for inner-shell ionization by electron and positron impact, Phys. Rev. A 67 (2003) 062710, http://dx.doi.org/10.1103/PhysRevA.67.062710.

[12] D. Bote, F. Salvat, Calculations of inner-shell ionization by electron impact with the distorted-wave and plane-wave Born approximations, Phys. Rev. A 77 (2008) 042701, http://dx.doi.org/10.1103/PhysRevA.77.042701.

[13] C.C. Montanari, J.E. Miraglia, Electron-impact multiple ionization of Ne, Ar, Kr and Xe, J. Phys. B: At. Mol. Opt. Phys. 47 (10) (2014) 105203, http://dx.doi.org/10.1088/0953-4075/47/10/105203.

[14] A. Bar-Shalom, M. Klapisch, J. Oreg, HULLAC, an integrated computer package for atomic processes in plasmas, J. Quant. Spectrosc. Radiat. Transfer 71 (2–6) (2001) 169–188, http://dx.doi.org/10.1016/S0022-4073(01)00066-8.

[15] M. Oswal, S. Kumar, U. Singh, S. Singh, G. Singh, K.P. Singh, D. Mehta, A.M.P. Mendez, D.M. Mitnik, C.C. Montanari, D. Mitra, T. Nandi, Experimental and theoretical L-shell ionization cross sections of heavy atoms by impact of Si ions, Radiat. Phys. Chem. 176 (2020) 108809, http://dx.doi.org/10.1016/j.radphyschem.2020.108809.

[16] M. Oswal, S. Kumar, U. Singh, G. Singh, K. Singh, D. Mehta, D. Mitnik, C. Montanari, T. Nandi, L x-ray production cross sections in high-Z atoms by 3–5 MeV/u silicon ions, Nucl. Instrum. Methods Phys. Res. B 416 (2018) 110–118, http://dx.doi.org/10.1016/j.nimb.2017.11.025.

[17] S. Chatterjee, S. Kumar, S. Kumar, M. Oswal, B. Mohanty, D. Mehta, D. Mitra, A.M.P. Mendez, D.M. Mitnik, C.C. Montanari, L. Sarkadi, T. Nandi, Understanding the mechanisms of L-shell x-ray emission from Os atoms bombarded by 4–6 MeV/u fluorine ion, Phys. Scr. 97 (4) (2022) 045405, http://dx.doi.org/10.1088/1402-4896/ac5711.

[18] G.P. Williams, Electron binding energies of the elements, in: W.M. Haynes (Ed.), CRC Handbook of Chemistry and Physics, 95, CRC Press, 2014, pp. 200–205.

[19] D. Bote, F. Salvat, A. Jablonsky, C. Powell, Cross sections for ionization of K, L and M shells of atoms by impact of electrons and positrons with energies up to 1 GeV: Analytical formulas, At. Data Nucl. Data Tables 95 (2009) 871–909, http://dx.doi.org/10.1016/j.adt.2009.08.001.

[20] C. Froese Fischer, General Hartree-Fock program, Comput. Phys. Comm. 43 (3) (1987) 355–365, http://dx.doi.org/10.1016/0010-4655(87)90053-1.

[21] C.C. Montanari, P.A. Miranda, E. Alves, A.M.P. Mendez, D.M. Mitnik, J.E. Miraglia, R. Correa, J. Wachter, M. Aguilera, N. Catarino, R.C. da Silva, Stopping power of hydrogen in hafnium and the importance of relativistic $4f$ electrons, Phys. Rev. A 101 (2020) 062701, http://dx.doi.org/10.1103/PhysRevA.101.062701.

[22] C.N. Chang, L-subshell ionization cross section for tunsgten at low energies, Phys. Rev. A 19 (1979) 1930, http://dx.doi.org/10.1103/PhysRevA.19.1930.

[23] T.L. Hardt, R.L. Watson, L-shell ionization of intermediate- and high-Z elements by alpha particles, Phys. Rev. A 14 (1976) 137, http://dx.doi.org/10.1103/PhysRevA.14.137.

[24] H.V. Rahangdale, M. Guerra, P.K. Das, S. De, J.P. Santos, D. Mitra, S. Saha, Determination of subshell-resolved L-shell-ionization cross sections of gold induced by 15–40-keV electrons, Phys. Rev. A 89 (2014) 052708, http://dx.doi.org/10.1103/PhysRevA.89.052708.

[25] S.F. Barros, V.R. Vanin, N.L. Maidana, M.N. Martins, J.A. García-Álvarez, O.C.B. Santos, R.C. L., M. Koskinas, J.M. Fernández-Varea, Ionization cross sections of the Au L subshells by electron impact from the L_3 threshold to 100 keV, J. Phys. B: At. Mol. Opt. Phys. 51 (2018) 025201, http://dx.doi.org/10.1088/1361-6455/aa98d3.

[26] S.F. Barros, V.R. Vanin, N.L. Maidana, A.A. Malafronte, J.M. Fernández-Varea, M.S. Pindzola, Experimental and theoretical L-subshell ionization cross sections for $_{83}$Bi by electron impact from the L3 threshold to 100 keV, Phys. Rev. A 105 (2022) 012818, http://dx.doi.org/10.1103/PhysRevA.105.012818.

[27] M. Pajek, A.P. Kobzev, R. Sandrik, A.V. Skrypnik, R.A. Ilkhamov, S.H. Khusmurodov, G. Lapicki, M-shell x-ray production by 0.6–4.0-MeV protons in ten elements from hafnium to thorium, Phys. Rev. A 42 (1990) 261–272, http://dx.doi.org/10.1103/PhysRevA.42.261.

[28] K. Ishii, S. Morita, H. Tawara, H. Kaji, T. Shiokawa, M-shell ionization of Au, Bi, and U by protons and helium ions in the MeV region, Phys. Rev. A 11 (1975) 119, http://dx.doi.org/10.1103/PhysRevA.11.119.

[29] M.H. Chen, B. Crasemann, H. Mark, Relativistic M-shell radiationless transitions, Phys. Rev. A 21 (1980) 449–453, http://dx.doi.org/10.1103/PhysRevA.21.449.

[30] E.J. McGuire, Atomic M-shell Coster-Kronig, Auger, and radiative rates, and fluorescence yields for Ca-Th, Phys. Rev. A 5 (1972) 1043–1047, http://dx.doi.org/10.1103/PhysRevA.5.1043.